Dynamic self-assembly of magnetic particles on the fluid interface: Surface-wave-mediated effective magnetic exchange

A. Snezhko, I. S. Aranson, and W.-K. Kwok
Materials Science Division, Argonne National Laboratory, 9700 South Cass Avenue, Argonne, Illinois 60439, USA
(Received 29 November 2005; published 28 April 2006)

We report on studies of dynamic self-assembled structures induced by a vertical alternating magnetic field in an ensemble of magnetic particles suspended on a liquid surface. We find the formation of nontrivially ordered dynamic snakelike objects in a certain range of field magnitudes and frequencies. In order to probe the properties of the "snakes," we study their magnetic response to in-plane magnetic field applied at different angles with respect to its axis. The segments of the snake exhibit long-range antiferromagnetic ordering mediated by the surface waves, while each segment is composed of ferromagnetically aligned chains of microparticles. We propose a simple phenomenological model where the effect of surface waves is replaced by an effective exchange interaction to describe the observations. In the framework of the proposed model, the effective exchange constant corresponding to different regimes of magnetic driving was extracted from the experimental data.

DOI: 10.1103/PhysRevE.73.041306 PACS number(s): 45.70.−n, 05.65.+b, 75.50.Tt

I. INTRODUCTION

A generic out-of-equilibrium dissipative system subject to a periodic homogeneous driving force develops coherent large-scale structures [1]. The recent interest in pattern formation occurring at all lengthscales in condensed matter, biological, and chemical systems is driven by the perspective to understand the nature of the dynamic self-assembly [2]. Complex wave patterns on the surface of fluid subject to vertical vibration have intrigued researchers since their discovery by Faraday in 1831 [3]. Square and more complicated standing wave structures have proved pivotal for understanding of fluid instabilities and principles of self-organization in nature [4]. Recently, analogues of Faraday waves were discovered in a broad class of systems, from granular materials [6] to ferrofluids [7–10]. A similar mechanism can be used for controlled self-organization of magnetic microparticles into complex architectures with the resulting structure and magnetic properties effectively controlled by the parameters of the external driving magnetic fields. Self-assembly of interacting particles in two-dimensional or three-dimensional ordered patterns is one of the promising ways of creating periodic templates for a broad range of nanotechnological applications (e.g., lithographic masks) and comprise a nonorthodox approach to fabrication of photonic-band crystals with tunable properties [11].

In a recent publication [12], we reported on the discovery of a remarkable dynamic multisegmented snakelike structure self-assembled from an ensemble of magnetic microparticles suspended on the surface of fluid and energized by an alternating vertical magnetic field. Here, we focus on the magnetic properties of the snakes in detail. We have found that these structures appear due to the dynamic coupling between the surface waves generated at a liquid interface and the collective response of particles to an external magnetic driving. The parameters of the self-assembled structures can be fine-tuned by changing the frequency and the amplitude of the driving field. The generated snakelike objects exhibit unique magnetic structure: long-range antiferromagnetic ordering between segments accompanied by a ferromagnetic ordering of chains composed of microparticles within each segment. We show that the effect of the surface wave on the creation of the reported multisegment magnetic structures can be modeled at the phenomenological level by introducing an effective magnetic exchange interaction between the segments of the snakelike structure. The theoretical predictions of the model are in good agreement with the experiments. In the framework of our model, we could extract the effective exchange constant corresponding to different regimes of magnetic driving from the experimental data.

The structure of the paper is as follows. In Sec. II we discuss the details of the experimental setup and present the main experimental results. In Sec. III we present our phenomenological model of pattern formation for a system of magnetic particles on a liquid surface under an external magnetic driving force. In Sec. IV we investigate the magnetic properties of the snakes in the framework of an effective exchange model. In Sec. V we compare the experimental data with our theoretical predictions. Open questions are discussed in Sec. VI.

II. EXPERIMENT

Our experimental setup is comprised of magnetic 90 μm nickel spheres floating on water. The spheres are small enough to be supported by surface tension. A cylindrical container (50 mm in diameter) with the floating magnetic microspheres is placed in a vertical alternating (ac) magnetic field $H_{ac}=H_0\sin(2\pi ft)$, where H_0 and f are the amplitude and frequency of the applied field, respectively. The magnetic field is produced by an electromagnetic coil (170 mm in diameter) capable of creating vertical magnetic fields up to 120 Oe. An additional in-plane dc magnetic field H_{dc} (up to 30 Oe), can be applied with a pair of Helmholtz coils to probe the magnetic properties of the self-assembled structures. The saturated magnetic moment per particle is 2×10^{-4} emu at a

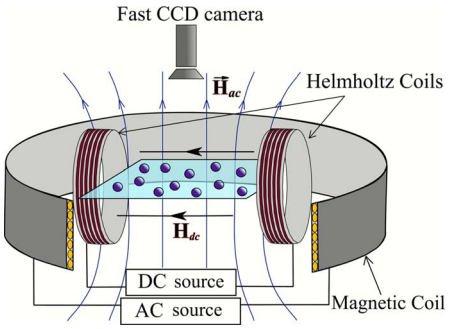

FIG. 1. (Color online) Schematic view of the experimental setup. See text for details.

saturation field of about 4 kOe. The magnetic moment per particle in the driving fields used in the experiments (~100 Oe) is one order of magnitude smaller. The motion of the individual particles in the container is monitored with a high-speed camera (a schematic view of the experimental setup is shown in Fig. 1). The inhomogeneity of the driving magnetic field in our setup is negligible since the magnetic force associated with the vertical field gradient per particle on the liquid surface in the container is less than 1% of its gravitational force.

Magnetic microparticles subjected to a uniform constant magnetic field experience a torque, forcing their magnetic moment to be aligned with the applied magnetic field. When aligned with the field, the microparticles start to experience a strong dipole-dipole repulsion resulting in a formation of a two-dimensional lattice structure of particles [see Fig. 2(a)] floating on the surface of liquid [13–15]. The application of an alternating (ac) magnetic field leads to the creation of new nontrivial snakelike structures. The appearance of these self-organized structures is attributed to the collective response of the magnetic particles to an external driving and their strong interaction with the surface of the surrounding liquid. In the course of magnetic moment alignment of the particles with the driving magnetic field, the particles drag the surrounding fluid and produce local oscillations of the water's surface, thereby affecting other particles. If the particles happen to be close enough to each other, the head-to tail dipole-dipole attraction (the magnetic field magnitude generated by the particle in the vicinity of its surface exceeds 200 Oe) overcomes the repulsion force between particles caused by the external field. Consequently, a chain of particles is formed with the resulting magnetic moment pointing along the chain. This chain produces wave-like local oscillations which facilitate the self-assembly process: parallel to the surface of the wave component of the magnetic field further promotes chaining (the sketch of the coupling mechanism between chains and a surface wave is shown as inset in Fig. 3). Remarkable self-organized multisegment structures emerge as a result of the collective interaction between the particles driven by an external ac magnetic field and the water's surface. Some examples of the self-assembled snakelike structures generated in an ensemble of 90 μm nickel spherical particles at different driving frequencies are presented in Fig. 2 (see Ref. [16] for movie demonstrating dynamic snake-like magnetic structures). The generated structures are dynamic

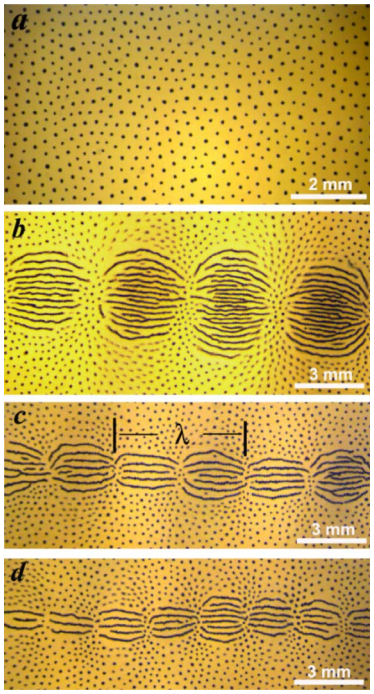

FIG. 2. (Color online) Panel (a): pattern generated by a static magnetic field (110 Oe magnitude). Panels (b), (c), and (d): Self-assembled multisegment snakelike structures generated by a vertical alternating 110 Oe magnetic field. The size of the segments is determined by the magnetic field frequency. (b), (c) and (d) represent structures generated at 30, 50, and 70 Hz, respectively.

and exist only while there is an external driving field. Once formed, the multisegment structures are quite stable, provided the driving force is unchanged and the excitation frequency is below some critical value as discussed below. However, strong mechanical excitation of the water surface could destroy the structure and the system subsequently undergoes a transition to the lattice state similar to the one shown in Fig. 2(a).

The primary mechanism of the snake formation is related to a resonant collective response of the water surface to the periodic driving force generated by the oscillating chains of particles. The antiferromagnetic alignment between the section provides a very effective coupling between oscillations of the chains and surface waves: in the course of alignment of their magnetic moment the neighboring sections induce surface wave oscillations as shown in Fig. 3 (inset). Consequently, the surface waves oscillate at the frequency of the applied field.

The excitation of surface waves by oscillating magnetic particles responding to an alternating magnetic field is analogous to Faraday waves in ferrofluids and is the primary mechanism for the formation of these snakelike structures. The characteristic length scale of the self-assembled structures is closely related to the parameters of the excited surface waves and the frequency of excitation. Figure 3 shows the full period of the structure as a function of the external field frequency (full period includes two sections of the snake). Apparently, the period of the generated structure quite closely follows the dispersion relation for the surface

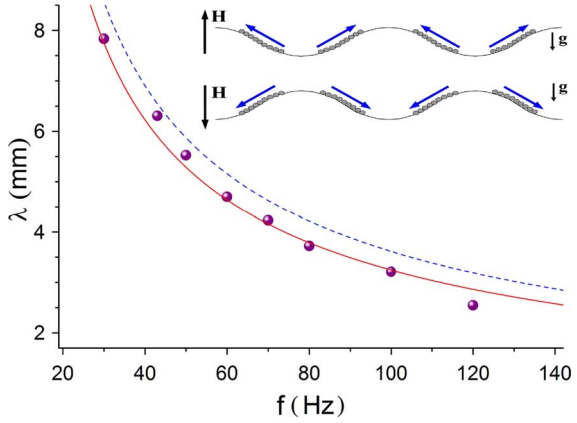

FIG. 3. (Color online) Full period of the self-organized structure λ versus frequency of the driving external magnetic field f. Symbols show experimental data for magnetic field amplitude of 110 Oe. The dashed line represents the dispersion relation for the surface waves in water with surface tension taken into account (no fitting parameters). The solid line represents the dispersion relation for surface waves in water, accounting for the magnetic contribution [see Eq. (1)] with $\alpha=0.28$. Inset: Sketch of coupling between chains and the surface wave. Arrows indicate magnetic moment orientations in the segments.

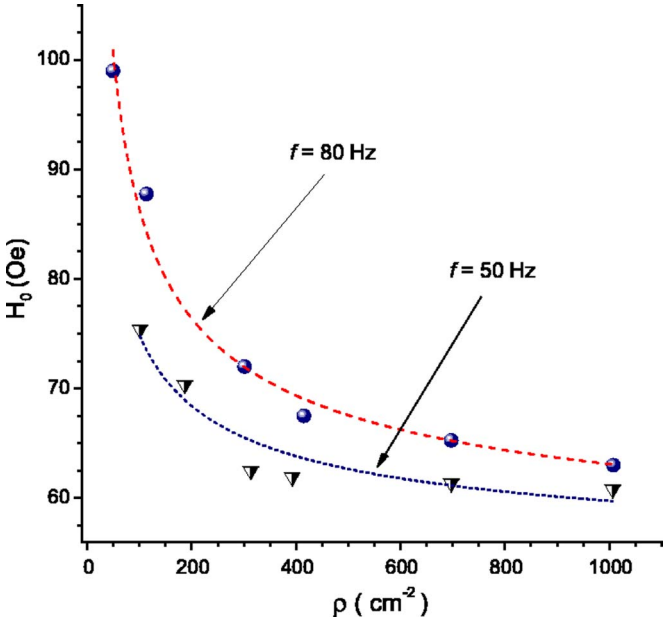

FIG. 4. (Color online) Critical field amplitude of the "snake" formation as a function of a surface particle's density (number of particle per unit area of the water/air interface). The data is shown for two driving frequencies 50 and 80 Hz. Dashed lines represent fits to the expression $H_0=A+B/\sqrt{\rho}$.

waves in water [17] when accounting for the surface tension and magnetic contribution

$$f^2 = \frac{g}{2\pi\lambda} + \frac{2\pi T}{\rho\lambda^3}(1-\alpha). \quad (1)$$

Here, ρ is the density of water, g is the gravitational acceleration, T denotes the water surface tension constant, and α is a phenomenological parameter accounting for a modification of the effective surface tension of liquid due to the presence of magnetic particles. Apparently, the magnetic contribution should introduce some "softening" of the liquid's surface due to the repulsive dipole-dipole interaction between neighboring magnetic particles floating on the surface.

The number of chains in the segment could be tuned by the frequency of the applied alternating magnetic field: decrease in the driving frequency results in an increase in the number of ferromagnetic chains within a segment, see Fig. 2. There is a critical driving field amplitude below which no snake-like structures could be generated. The value of the critical field is strongly dependent on the external driving frequency and number of magnetic particles in the ensemble: higher field amplitude is required to create a snake structure when working at a higher driving frequency or smaller number of particles in an ensemble. The critical field amplitude as a function of particle surface density is plotted in Fig. 4 for two different driving frequencies. The dashed lines in the Fig. 4 are fits of the experimental data to the function $H_0=A+B/\sqrt{\rho}$ (A and B here are parameters) and provide a good description of the dependencies observed in the experiments.

As mentioned above, the snakes have a unique magnetic ordering: while within each segment the chains are ferromagnetically ordered, the neighboring segments have antiferromagnetic alignment. Obviously, the chain formation is driven by a magnetic dipole-dipole interactions that govern the local arrangement of the magnetic particles [19,20]. The interchain distance within a segment is apparently determined by the repulsion of parallel dipole structures. The segments, however, are antiferromagnetically aligned: the total magnetic moment per segment reverses its direction from one segment to the next. To demonstrate this point, a small in-plane dc magnetic field was applied to the self-organized snake structure. The response of the self-organized structures (generated with a 50 Hz driving magnetic field and 110 Oe amplitude) to an in-plane static magnetic field (2 Oe) is illustrated in Fig. 5. The dc in-plane magnetic field applied perpendicular to the snake's long axis induces a zigzag ordering of the segments indicative of antiferromagnetic arrangement of the neighboring sections. Thus, the entire structure represents a multisegment magnetic object with short range ferromagnetic ordering (within the segments) and long range antiferromagnetic arrangement (between segments). A dc in-plane field applied parallel to the snake structure leads to a gradual decrease in the chain number with field amplitude in segments with unfavorable magnetic moment orientation with respect to the in-plain field. A snake in the parallel in-plane magnetic field orientation where only one orientation of the segments survived is shown in Fig. 6.

The snakes create large-scale vortex structures (see Ref. [16]), most likely due to the interaction between surface waves and the hydrodynamic modes of the container. These vortices are fundamentally different from the vortices formed in the system of spinners excited by the rotating magnetic field [5]. In our system, the vortices are the result of spontaneous symmetry breaking due to some form of dynamic instability, whereas in Ref. [5] the vortices are produced by rotation of the field in a prescribed direction. Certainly, these

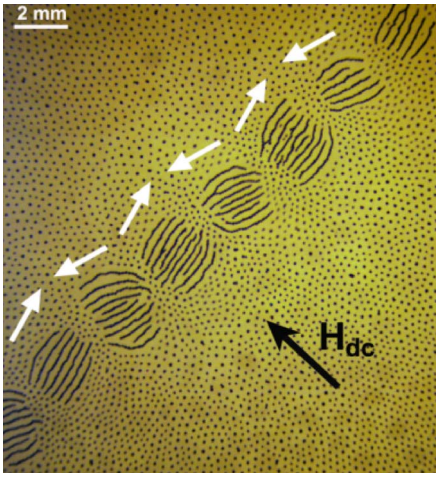

FIG. 5. (Color online) Magnetic response of the "snake" on the transversal in-plane dc magnetic field of 2 Oe. Structure was generated at $f=50$ Hz, $H_0=110$ Oe driving vertical magnetic field. White arrows designate the magnetic moment direction at corresponding segments. The resulting zigzag structure indicates antiferromagnetic ordering of the segments.

vortices deserve deep investigation, however, in this paper we will focus on the magnetic properties of the observed structures and we leave the study of these unique vortices to a later report.

III. MODEL OF PATTERN FORMATION

The self-localization of the snake structures can be understood in the framework of an amplitude equation for parametric waves coupled to the conservation law equation describing the evolution of the magnetic particle density. While parametrically excited waves are well known in the context of magnetic fluids, we emphases the large difference between our system and ferrofluids. In ferrofluids, the density variations of magnetic nanoparticles is small compared to the average density. In contrast, in our system the density of microparticles floating on the fluid surface exhibits considerable oscillations, leading sometimes to the formation of particle-free regions. Consequently, in our case the density of particles is an independent parameter responsible for the self-localization of the parametric waves.

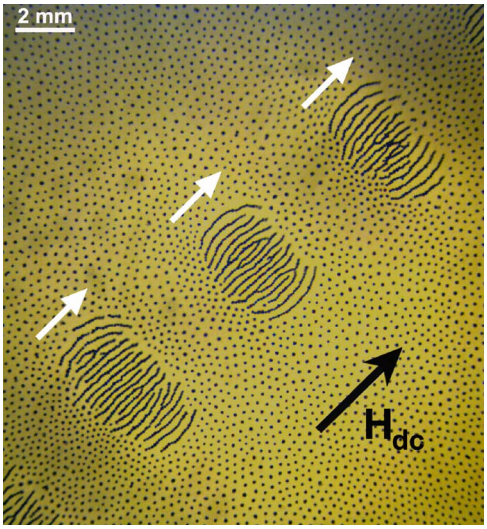

FIG. 6. (Color online) Magnetic response of the snake on the in-plane dc magnetic field of 10 Oe applied parallel to the structure's axis. Structure was generated at $f=50$ Hz, $H_0=110$ Oe driving magnetic field. White arrows designate the magnetic moment direction at corresponding segments. Sublattice with unfavorable magnetic moment orientation is completely eliminated. Magnetic period now coincides with the period of the surface wave.

We previously used a similar approach to describe self-localized structures (oscillons) in vibrating granular layers [18]. We describe our system with a set of two coupled equations

$$\partial_t \psi = -(1-i\omega)\psi + (\varepsilon + ib)\nabla^2\psi - |\psi|^2\psi + \gamma\psi^*\phi(\rho),$$

$$\partial_t \rho = D\nabla^2\rho - \beta\nabla(\rho\nabla|\psi|^2). \quad (2)$$

The first equation (2) is a paradigm model for parametrically-excited surface waves [ψ is the complex amplitude of the surface wave $\sim\psi\exp(i\omega t)+\text{c.c.}, \omega=2\pi f/f_0$] that includes parametric driving $\gamma\psi^*$ (with driving amplitude γ function of magnetic field amplitude H_0, see below), nonlinear damping $|\psi|^2\psi$. Here the original driving frequency f of the ac magnetic field is scaled by the (arbitrary) reference frequency f_0, time t is normalized by the reference frequency time scale $1/(2\pi f_0)$, and length is scaled by the characteristic length scale l_0 obtained from the dispersion relation for surface waves Eq. (1). For example, one obtains from the dispersion relation $l_0 \approx 6$ mm for a reference frequency $f_0=40$ Hz. The linear operator in the equation for ψ is obtained by expansion of the dispersion relation Eq. (1) near the frequency ω and corresponding wavenumber k (here $k\approx\sqrt{\omega/b}$). The viscous dissipation is modeled by $\epsilon\nabla^2\psi$.

The second equation (2) expresses the conservation law for particle number density ρ. Here, D is a diffusion coefficient and β is the amplitude of the advection term describing the concentration of particles by waves.

The effect of forcing the waves by magnetic field is modelled by the term $\gamma\psi^*\phi(\rho)$. On symmetry grounds, one concludes that the driving amplitude γ should be proportional to the square of the magnetic field amplitude H_0, $\gamma\sim H_0^2$, since for pure ac applied magnetic field H the system is not sensitive to the sign reversal of H. This symmetry can be destroyed by applying an additional dc magnetic field, but we leave this interesting question for further investigation. The function ϕ, which phenomenologically describes the dependence of the forcing term on the density of particles, is proportional to ρ for small densities and saturates for larger densities. For simplicity, we took $\phi=\rho-0.3\rho^2$. This density dependence accounts for the fact that the effect of forcing vanishes for low particle densities ($\rho\to 0$) and saturates for higher densities. It is consistent with our experimental observation of the dependence of the critical field H_0 for a snake formation on the number of particles, see Fig. 4. From the linear stability analysis of the trivial (nonoscillating) state $\psi=0, \rho=\rho_0=\text{const}$ one obtains from Eqs. (2) that parametric

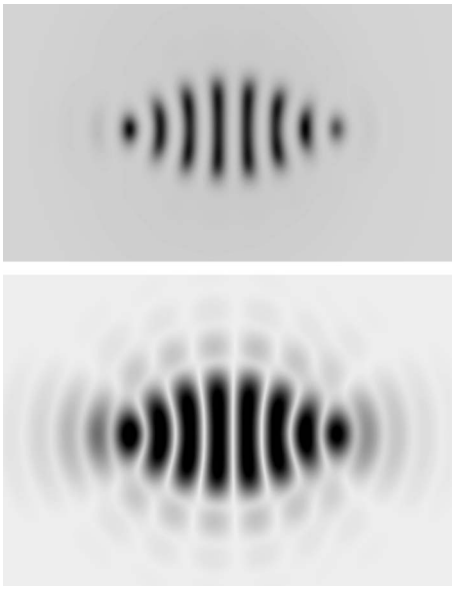

FIG. 7. Pattern obtained by numerical modelling. Top panel: Pattern formed by magnetic particles at the liquid surface. The intensity of the dark color is proportional to the density of magnetic particles. Bottom panel: Hydrodynamic field induced by the collective response of particles to the external magnetic driving. Dark color intensity is proportional to the amplitude of the generated surface waves. Parameters in Eq. (2) are $\varepsilon=1, b=2, \gamma=2.5, D=1, \beta=8.5, \omega=3$, in domain of 100×100 dimensionless units.

instability occurs at the optimal wavenumber $k=k^*=\sqrt{(\omega b-\varepsilon)/(\varepsilon^2+b^2)}$ and at the critical driving amplitude $\gamma=\gamma_c$ given by the expression (see for comparison Ref. [18])

$$\gamma_c\phi(\rho_0)=\frac{\omega\varepsilon+b}{\sqrt{\varepsilon^2+b^2}}. \tag{3}$$

Thus, for small densities $\rho=\rho_0\to0$ we obtain from Eq. (3) that the critical value of γ_c for parametric instability behaves as $\gamma_c\sim1/\rho_0$. Since $\gamma\sim H_0^2$, we obtain from Eq. (3) $H_0\sim1/\sqrt{\rho_0}$, which is consistent with our experimental observations (see Fig. 4).

Equations (2) describe the formation of localized snakelike structures over a wide range of parameters. However, contrary to the situation considered in Ref. [18], the self-localization occurs due to the fact that surface oscillations can herd the magnetic particles into some regions and reduce their concentration in neighboring areas. Since the driving force magnitude is proportional to the local particle concentration, surface wave excitation occurs only in particle-rich areas and decays in the depleted areas. A typical pattern obtained by numerical modeling is shown in Fig. 7 (top panel).

While this continuum approach gives some insights on the self-localization mechanism, it certainly ignores the internal filamentary structure of the snake. In order to address the fine structure of the segments, one needs to find an appropriate description for the discrete particles' level, using formalisms such as the Newton-type equations for individual particles coupled to the continuous hydrodynamic field. Furthermore, our approach does not describe the formation of the large-scale vortex motion (see Ref. [16]). We believe that these phenomenon can be modeled in the framework of a modified Eq. (2) coupled to an additional mean flow hydrodynamic mode.

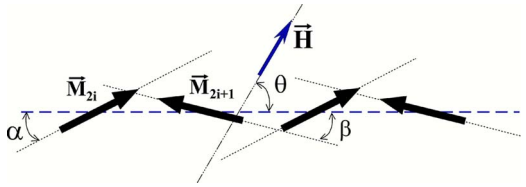

FIG. 8. (Color online) Model of the "snake" structure. Bold dashed line represents the axis of the structure; θ is an angle between the structure axis and an external in-plane magnetic field; α and β are deviations angles induced by the external magnetic field in corresponding sublattices of the structure.

IV. MAGNETIC STRUCTURE OF THE "SNAKE": SURFACE WAVE ASSISTED EFFECTIVE MAGNETIC EXCHANGE INTERACTION

Apparently, the mechanism governing the antiferromagnetic ordering of segments comes from the induced surface waves, since pure magnetic interactions make the snakelike structure energetically unfavorable. In this sense, the surface wave assistance in the creation of the multisegment snake structures is analogous to an effective magnetic exchange interaction between neighboring segments. In order to estimate this effective interaction we consider the segments of the snake structure as point dipoles. A schematic sketch of such a structure is plotted in Fig. 8. The corresponding energy term related to the effective exchange interaction between neighboring segments i and j reads $2J\vec{M}_i\vec{M}_j$ [21]. Here, J is some effective exchange constant related to the properties of the induced surface wave that are in turn functions of the liquid properties and external driving parameters. $\vec{M}_i$ and $\vec{M}_j$ are effective magnetic moments of the neighboring segments. In this simplified model, the total magnetic energy E of a snake subjected to an external in-plane magnetic field $\vec{H}_{\text{ext}}$ could be written in the following form:

$$E=\sum_{i=1}^{N}\sum_{\substack{j=1\\j<i}}^{N}\left(2J_{ij}\vec{M}_i\vec{M}_j+\frac{\vec{M}_i\vec{M}_j}{r_{ij}^3}-\frac{3(\vec{M}_i\vec{r}_{ij})(\vec{M}_j\vec{r}_{ij})}{r_{ij}^5}\right)-\vec{H}_{\text{ext}}\sum_{i=1}^{2N}\vec{M}_i. \tag{4}$$

Here, in addition to the magnetic exchange energy, we took into account the dipole-dipole interactions between the segments. $2N$ is the number of segments in the snake structure. We will assume for further calculations, only the effective exchange interactions of the nearest neighbors. Thus, in the limit of an infinitely long structure, the energy of the snake per segment in the presence of an external in-plane magnetic field could be derived in the following form:

$$E_s = m^2\Bigg[-4J\cos(\alpha+\beta) - \frac{H_{\text{ext}}}{2m}\{\cos(\Theta-\alpha)-\cos(\Theta+\beta)\} - \frac{2}{a^3}\langle A_1\cos(\alpha+\beta) - 3A_1\cos(\alpha)\cos(\beta) \quad - A_2\rangle - \frac{3A_2}{a^3}[\cos^2(\alpha)+\cos^2(\beta)]\Bigg]. \tag{5}$$

Here, m is an effective magnetic moment per segment of the structure; a is the distance between neighboring moments (apparently, $a=\lambda/2$); Θ designates the angle between external in-plane magnetic field and the axis of the snake structure (see Fig. 8); α and β denote deviation angles between the snake's axis and the effective moments of the segments belonging to different sublattices under the influence of the in-plane magnetic field. Here we assume that regardless of the sublattice the magnetic moment per segment is not a function of the external in-plane magnetic field. Such an assumption is quite reasonable for small in-plane magnetic fields when the internal structure of the segments remains unaffected. However, at high enough fields, the segments of the structure are strongly affected and the effective magnetic moment per segment becomes a function of the field as well as the sublattice (one sublattice increases its effective moment at the expense of another; see Fig. 6). Constants A_1 and A_2 in Eq. (5) reflect the long range nature of the dipole-dipole interactions and simply represent the contribution of the dipole-dipole interactions to the energy $A_1=\Sigma_0^\infty \frac{1}{(2n+1)^3} \simeq 1.05180$ and $A_2=\Sigma_1^\infty \frac{1}{(2n)^3} \simeq 0.15026$. One should put $A_1=1$ and $A_2=0$ for the case when only the nearest neighbors' dipole-dipole interactions are taken into account.

The deviation angles α and β are determined from the conditions of the energy minima

$$\partial E_s/\partial\alpha = 0,$$

$$\partial E_s/\partial\beta = 0. \tag{6}$$

These conditions result in a set of two coupled nonlinear equations (7) with respect to the deviation angles α and β which can be solved numerically for an arbitrary orientation of the external in-plane magnetic field to the axis of the snake structure:

$$8J\sin(\alpha+\beta) - \frac{H_{\text{ext}}}{m}\{\sin(\Theta-\alpha)+\sin(\Theta+\beta)\} - \frac{2}{a^3}[2A_1\sin(\alpha+\beta) - 3A_2\{\sin(2\alpha)+\sin(2\beta)\}] = 0,$$

$$\frac{H_{\text{ext}}}{m}[\sin(\Theta-\alpha)-\sin(\Theta+\beta)] - \frac{6}{a^3}\{A_2[\sin(2\alpha)-\sin(2\beta)] - 2A_1\sin(\alpha-\beta)\} = 0. \tag{7}$$

In the particular case when the applied in-plane magnetic field direction is perpendicular to the structure's axis, the set of Eq. (7) can be solved analytically. Since α is equal to β in this case, the corresponding deviation angle is determined by

$$\sin\alpha = \frac{H_{\text{ext}}}{4m[4J-(A_1-3A_2)/a^3]}. \tag{8}$$

Apparently, there is a critical magnitude of the in-plane magnetic field above which the snake structure with antiferromagnetic arrangement is no longer sustainable. For a transversal direction of the in-plane dc field this critical field magnitude is defined by a condition $\sin(\alpha)=1$ and results in a simple analytical expression $H_c=4m[4J-(A_1-3A_2)/a^3]$. Above H_c the system should transform to a segmented structure with a single orientation of magnetic moments (similar to one shown in Fig. 6). Indeed, such transitions were observed in the experiments. In the case of an arbitrary in-plane magnetic field orientation, the influence of the field on the segments belonging to different sublattices is nonsymmetric: one of the orientations (with positive projection of the segment's magnetic moment on the in-plane field direction) is more energetically favorable than the other. Consequently, the transformation to the single orientation snake proceeds gradually. As the critical field is approached, chains in segments with opposing magnetic moment orientation with respect to the applied in-plane field direction leave the segments, reorient and join segments with opposite magnetic moment. Such mechanism of magnetic moment redistribution between sublattices helps to significantly lower the energy of the structure and results in a broadening of the transition into the single-oriented structure with external in-plane magnetic field.

V. COMPARISON WITH EXPERIMENTS

In order to obtain the effective exchange constant, we applied different magnitudes of the in-plane magnetic field at some arbitrary angle θ to the snake structure's long axis. The deviation angles for both magnetically opposing sublattices were extracted from the data and plotted as a function of the magnitude of the dc in-plane magnetic field. In Fig. 9 the variation of the deviation angles α and β with the in-plane magnetic field magnitude is shown for a snake created with a vertical *ac* driving field ($H_0=80$ Oe, $f=50$ Hz). The in-plane dc magnetic field angle θ in the experiment shown in Fig. 5 was slightly varied in the range from 64° to 70°. To minimize the effect of the Earth's magnetic field, each measurement was taken twice with the in-plain field applied parallel and antiparallel to the Earth's magnetic field. The resulting curves were then fitted with solutions of Eq. (7) in order to extract the effective exchange constant. The outcome of this procedure is shown in Fig. 9 as solid lines. Clearly, our simplified model provides a rather good description of the observed experimental data indicating that the surface wave contribution to the creation of the antiferromagnetically ordered quasi one-dimensional structure could be well described by the introduction of some effective magnetic exchange interaction between neighboring segments of the structure. Since the properties of such an interaction are determined by the surface waves, a strong dependence on the external magnetic field driving frequency is expected. To probe the behavior of the exchange constant with respect to the frequency of the driving field, we carried out a series of

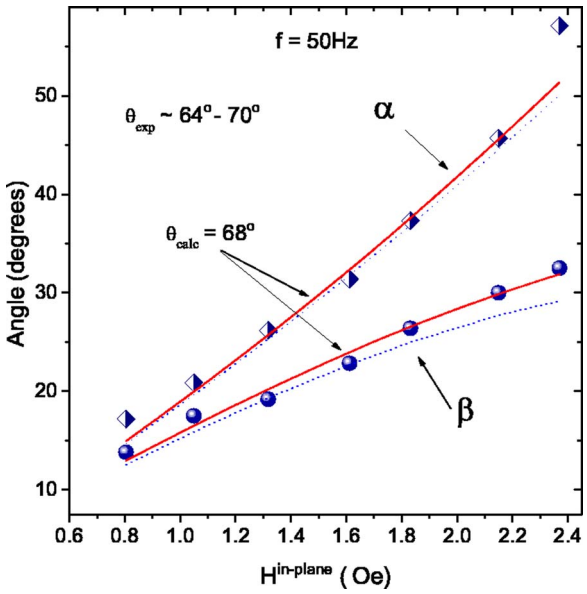

FIG. 9. (Color online) Deviation angles α and β corresponding to different magnetic sublattices of the "snake" as a function of external in-plane magnetic field amplitude. The angle θ between in-plain magnetic field and the structure's axis is in the range from 64° to 70°. Solid lines represent theoretical curves obtained for θ=68° in the framework of model where the surface wave assistance in the creation of antiferomagnetic ordering is replaced by some effective exchange interaction. Dotted lines are calculated curves for θ=65°.

experiments similar to ones described above for a set of different driving frequencies. The extracted exchange constants are plotted as a function of the driving frequency in Fig. 10. Clearly, the data indicates almost linear dependence of the exchange parameter on the driving field frequency. This result can explain the destruction of the snake structure at high driving frequencies. Let us consider the energy per segment of the unperturbed snake (zero in-plane magnetic field): $E_0=-4m^2[J-(A_1-A_2)/a^3]$. As we just pointed out the effective surface wave assisted magnetic exchange grows almost linearly with the frequency of the driving magnetic field. However, the competitive dipole-dipole contribution behaves as $1/a^3$, where the effective distance a is determined solely by the dispersion relation Eq. (1) ($a=\lambda/2$). Therefore, the dipole-dipole contribution to the energy evolves as a power of frequency higher than 2. Consequently, at some frequency, the dipole-dipole interaction overcomes the effective magnetic exchange interaction and the snake structure is destroyed. Such behavior was indeed observed in the experiments.

VI. CONCLUSIONS

We investigated the surface wave assisted self-assembly of magnetic structures in an ensemble of magnetic microparticles floating on a liquid subjected to periodic magnetic excitations. We found that excitation of the system by a vertical ac magnetic field results in the formation of a multi-segment magnetic structure whose characteristics are determined by the induced surface waves and can be fine-tuned by varying the frequency of the external driving magnetic field. The multi-segment structures exhibit long range antiferromagnetic ordering between segments, while each segment consists of ferromagnetically aligned chains of microparticles. We demonstrated that surface wave assisted creation of the antiferromagnetically ordered snake could be understood as a manifestation of an effective exchange interaction between the snake's segments mediated by the surface wave. Our proposed model provides a good description of the observed magnetic behavior of the dynamic self-assembled structures. Effective exchange constants corresponding to different regimes of driving were extracted from the experimental data.

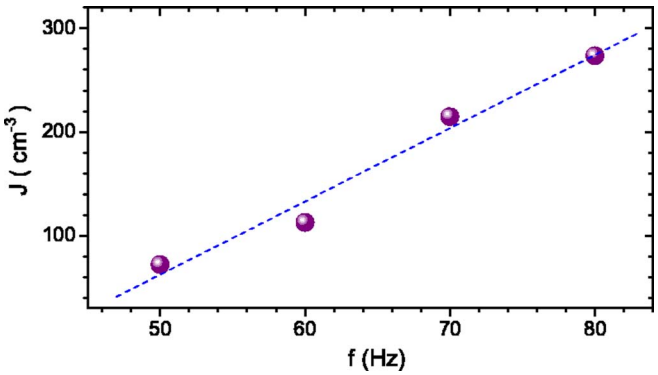

FIG. 10. (Color online) Effective exchange constant as a function of frequency of the external vertical magnetic field driving. Amplitude of the driving is 110 Oe. Dashed line is a linear fit of the data.

Many open questions remain for future extended studies. The mechanisms leading to the creation of vortices are not clear. One expects that the large-scale vortices could appear as a result of some nontrivial coupling between the parametrically-excited surface waves and the hydrodynamic modes of the container. However, additional experimental and theoretical studies are necessary to identify the mechanism of flow generation. Note that slowly rotating spiral patterns were observed in traditional Faraday wave experiments: vertically vibrated thin layer of viscous fluid [22]. The mechanism of large-scale flow generation was associated with the effect of the lateral walls of the container. We emphasize that in our system, the mechanism is entirely different and not related to boundary wall effects. The existing theory of pattern formation does not address the chain structure of snake's segments, it is highly desirable to extend it in many directions and couple continuum models with molecular dynamics simulations. The scalability of the snakes is a very intriguing issue. The reduction of the particle size below a micron may open opportunities for new nano-technology applications where self-assembly of nanoparticles is of particular interest.

ACKNOWLEDGMENTS

This research was supported by US Department of Energy, Grant No. W-31-109-ENG-38.

[1] M. C. Cross and P. C. Hohenberg, Rev. Mod. Phys. **65**, 851 (1993).
[2] G. M. Whitesides and B. Grzybowski, Science **295**, 2418 (2002).
[3] M. Faraday, Philos. Trans. R. Soc. London **121**, 299 (1831).
[4] A. Kudrolli and J. P. Gollub, Physica D **97**, 133 (1996).
[5] B. A. Grzybowski and G. M. Whitesides, Science **296**, 718 (2002).
[6] P. Umbanhowar, F. Melo, and H. L. Swinney, Nature (London) **382**, 793 (1996).
[7] J.-C. Bacri, A. Cebers, J. C. Dabadie, S. Neveu, and R. Perzynski, Europhys. Lett. **27**, 437 (1994).
[8] J.-C. Bacri, A. Cebers, J. C. Dabadie, and R. Perzynski, Phys. Rev. E **50**, 2712 (1994).
[9] V. G. Bastovoi and R. E. Rosensweig, J. Magn. Magn. Mater. **122**, 234 (1993).
[10] T. Mahr and I. Rehberg, Europhys. Lett. **43**, 23 (1998).
[11] J. Jannopoulos, R. Meade, and J. Winn, *Photonic Crystals* (Princeton University Press, Princeton, NJ, 1995).
[12] A. Snezhko, I. S. Aranson, and W.-K. Kwok (unpublished).
[13] E. Yablonovitch and K. M. Leung, Nature (London) **391**, 667 (1998).
[14] M. Golosovsky, Y. Saado, and D. Davidov, Appl. Phys. Lett. **75**, 4168 (1999).
[15] W. Wen, L. Zhang, and P. Sheng, Phys. Rev. Lett. **85**, 5464 (2000).
[16] See EPAPS Document No. E-PLEEE8-73-056605 for movie illustrating dynamical self-assembled multi-segment magnetic structures. For more information on EPAPS, see http://www.aip.org/pubservs/epaps.html
[17] L. D. Landau and E. M. Lifshits, *Fluid Mechanics* (Pergamon Press, New York, 1987).
[18] L. S. Tsimring and I. S. Aranson, Phys. Rev. Lett. **79**, 213 (1997).
[19] A. Snezhko, I. S. Aranson, and W.-K. Kwok, Phys. Rev. Lett. **94**, 108002 (2005).
[20] D. L. Blair and A. Kudrolli, Phys. Rev. E **67**, 021302 (2003).
[21] A. H. Morrish, *The Physical Principles of Magnetism* (John Wiley and Sons, New York, 1965).
[22] S. V. Kiyashko, L. N. Korzinov, M. I. Rabinovich, and L. S. Tsimring, Phys. Rev. E **54**, 5037 (1996).